4. ANKARA INTERNATIONAL AEROSPACE CONFERENCE **AIAC-2007-004**
10-12 September, 2007 - METU, Ankara

TIP-LEAKAGE VORTEX MINIMIZATION IN DUCTED AXIAL FANS USING NOVEL PRESSURE SIDE TIP PLATFORM EXTENSIONS

Cengiz CAMCI* and Ali AKTURK†
The Pennsylvania State University
Turbomachinery Aero-Heat Transfer Laboratory
University Park, PA, USA

ABSTRACT

Efficiency of an axial fan unit used in ducted fan based propulsion systems is closely related to its tip leakage mass flow rate and the level of tip/casing interactions. The present experimental study uses a stereoscopic Particle Image Velocimeter to quantify the three dimensional mean flow observed at just downstream of a ducted fan unit. After a comprehensive description of the tip leakage influenced fan exit flow, a number of tip treatments based on pressure side extensions are introduced. Various tip leakage mitigation schemes are introduced by varying the chordwise location and the width of the extension in the circumferential direction. The current study shows that a proper selection of the pressure side bump location and width are the two critical parameters influencing the success of tip leakage mitigation. Significant gains in axial mean velocity component are observed when a proper pressure side tip extension is used. It is also observed that a proper tip leakage mitigation scheme significantly reduces the tangential velocity component near the tip of the axial fan blade. Reduced tip clearance interactions are essential in improving the energy efficiency of ducted fan systems. Aeroacoustic gains are also possible. A reduction or elimination of the momentum deficit in tip vortex structures are also expected to reduce the adverse performance effects originating from the unsteady and highly turbulent tip leakage flows rotating against a stationary casing.

INTRODUCTION

The flow field between the stationary casing and rotor tip of an axial fan is complex because of complex interaction of the leakage flow, annulus wall boundary layer and rotor wake. Inherent pressure difference between the pressure side and suction side of blade tip section generates a tip leakage flow that is responsible from a substantial proportion of aerodynamic losses in in axial flow fans. That flow also rolls into a highly three dimensional tip leakage vortex with significantly turbulent and unsteady flow features in each passage. Tip leakage vortex is a complicated flow phenomena that is one of the dominant mechanisms of noise generation by unsteady interactions with fan blades. It is also one of the major energy loss sources for axial flow fan systems. Despite the close relation between the tip leakage flow and performance of axial fans, there has been limited amount of information about structure of leakage vortex in open literature [1-4].

The wake developed from an axial flow fan has a big influence on performance of the turbomachinery. It is a significant source of arodynamic loss and also affects the efficiency and vibration characteristics. References from [5] to [7] deal with extensive investigations of the wake flow features such as mean velocities, turbulence and decay characteristics

There has been many studies that all three components of mean velocity are measured with the help of SPIV. In general, exit flow field and tip region of the fan is measured by the help Stereoscopic Particle Image Velocimetry SPIV . SPIV is a powerful way of measuring three velocty components of flow field over

* Prof. of Aerospace Eng., The Pennsylvania State University, Turbomachinery Aero-Heat Transfer Lab., e-mail: cxc11@psu.edu
† Grad. Res. As. in Aerospace Eng. The Pennsylvania State University, Turbomachinery Aero-Heat Transfer Lab.

a determined area [8-12]. A comprehnsive discussion of the specific stereoscopic PIV technique used in this paper is given by Kahveci in [13].

Yoon and Lee et al. [14] investigated the flow structure around an axial flow fan using SPIV technique with two cameras.The time averaged PIV results clearly show the evolution and dissipation of tip vortices.

Yen and Lin et al. [15] analyzed exit flow performance and properties of an axial flow fan with winglet-blades at various impeller angles using SPIV. The velocity profiles show the the most stable and the best fan performace, resulting from the constraining shroud and winglet-blade, which increase the lift and reduce the drag.

The main objectives of the current study are summarized as follows:

1) To investigate the characteristics of tip leakage flow and tip vortex in an axial flow fan.
2) To eliminate the adverse effects of tip vortex by designing novel rotor tip geometries using pressure side extensions.
3) To reduce the momentum deficit in tip vortex structures.
4) Increasing the efficiency of axial fan systems.
5) To provide high quality mean flow data for further studies in aerocoustics of tip treated axial flow fans.

EXPERIMENTAL SET – UP

A test rig consisting of an axial flow fan, mock-up unit and electric drive system was designed to investigate the flow phenomena using a stereoscopic PIV system. The set-up has also provisions for seeding the fan flow field with a smoke generator using a fluidized bed located near the inlet section of the mock-up unit where a perforated plate is usually mounted. The electric motor driving the fan rotor is speed controlled by an AC inverter unit. Phase-locked SPIV measurements are triggered by using an optical once per revolution device located near the hub of the rotor inlet. An infrared beam is reflected from a highly reflective surface attached to the rotor hub. This once-per-rev pulse provides a phase-locked triggering of the SPIV data collection system. The relative position of the rotor can be adjusted accurately in relative to the position of the laser light sheet that contains the rectangular SPIV measurement area located at downstream of the rotor.

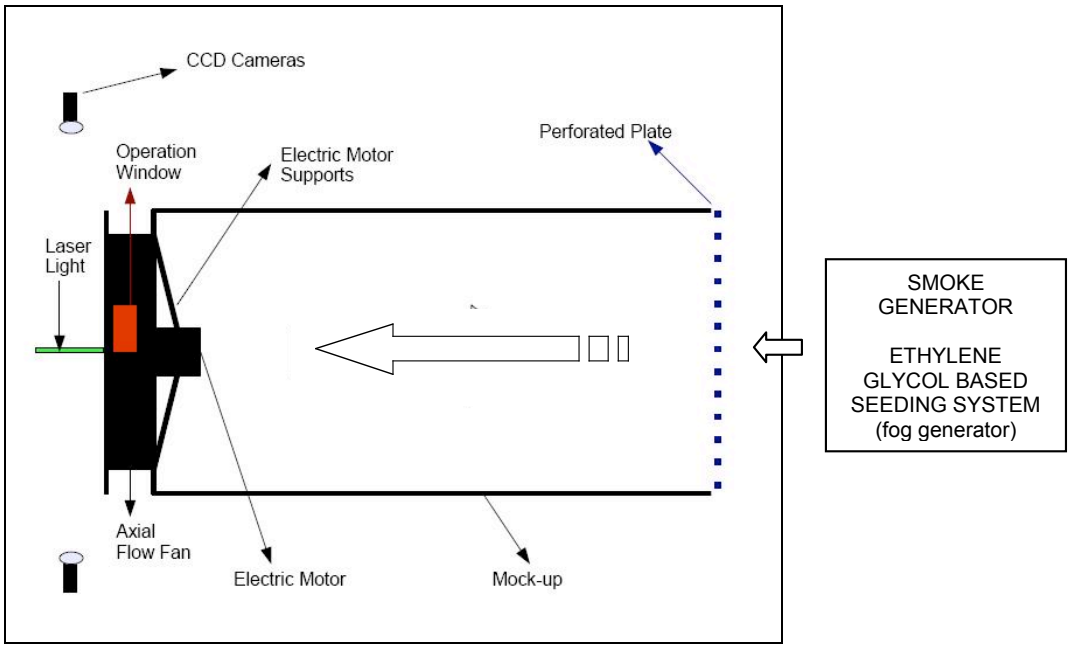

Figure 1: *Test Rig and Stereoscopic SPIV setup*
(the SPIV measurement plane is in horizontal plane)

Test Rig

Fig.2 shows the general characteristics of the seven bladed axial flow fan unit. The geometric specifications are also presented in Table 1. The axial flow fan unit is supported by a sheet metal mock-up system. A perforated plate at the inlet section of the mock-up is used for creating realistic fan loading conditions. The tip of the blades are modified through an "operation window" as shown in Figure 1. Only one blade tip out of seven blades is modified since the current SPIV system is capable of measuring in the immediate vicinity of a "selected" blade tip due to the phase-locked nature of the SPIV measurements.

The current rotor blades have serrated trailing edges for effective mixing of the blade boundary layers in the wake of each blade. The serrated trailing edges also provide an effective mixing of individual tip vortices with the wakes of the seven blades in the rotating frame of reference. It should be noted that the comparison of the flow with serrated trailing edges with smooth trailing edge flow is not the subject of the current paper. A comparative flow physics study of serrated trailing edges against smooth trailing edges is currently under progress in our laboratory.

Figure 2: *Axial flow fan as seen from the exit plane (perforated plate is also visible)*

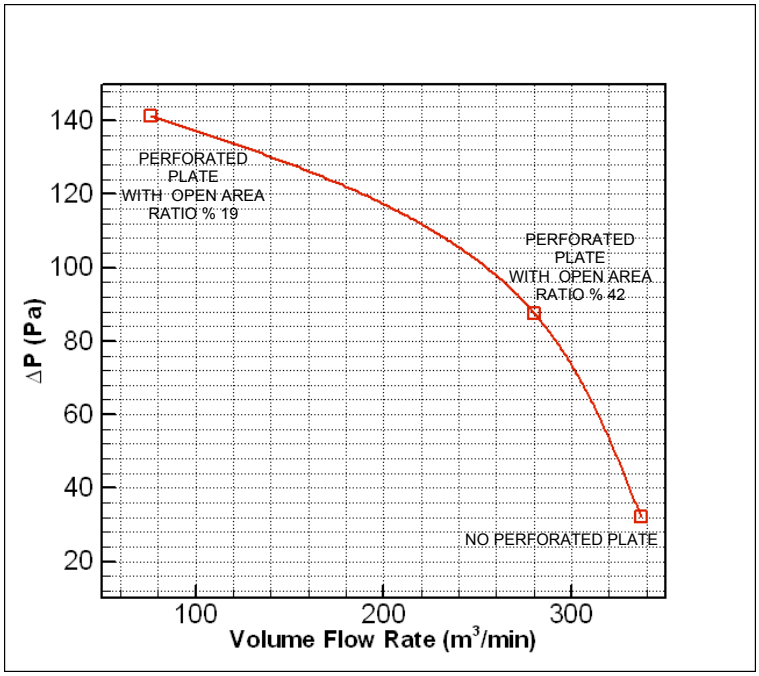

Figure 3: *Axial flow fan performance*

The performance of the fan unit is measured under three different loading conditions. The first performance point (140 Pa, 80 m^3/min) shown in Fig. 3 is obtained by using a perforated steel plate having an

open area ratio of 19.6 %. A second perforated plate using a slightly larger open area ratio 42.5% provides the middle point (280 m^3/min, 88 Pa) in the performance curve as shown in Fig. 3. The third point with the highest volumetric flow rate at 340 m^3/min is obtained when there is no perforated plate installed at the inlet section of the mock-up unit. Pressure change across the fan is measured by using Pitot static holes mounted on all four sides of the mock-up unit. Wall-static pressures from all four sides are averaged. For the mass flow rate measurements, a hot-wire anemometer is used at rotor downstream. Fig. 3 shows the performance curve of the fan unit.

Number of Blades	7
Tip Radius	15.15" (384.8 mm)
Hub Radius	5.00" (127.0 mm)
Tip Chord length	4.69" (116.8 mm)
Hub Chord length	5.89" (149.6 mm)
rpm	859
Tip Clearance	t = 0.1" (2.54 mm) t/h=0.1"/(15.15"-10.0") ≈ 1 % relative to blade height

Table 1: *Geometric parameters of the axial flow fan*

Stereoscopic PIV system

The PIV technique measures instantaneous velocity components of a flow field over a determined area [8-11]. Small particles are introduced into the fluid flow, and the region of interest is illuminated by the light sheet provided by short laser pulses lasting as short as a few nanoseconds. The subsequent step is the recording of the displacement of particles via one or two CCD cameras depending on the PIV technique used. As a summary, four basic steps should be mentioned in an experimental procedure:

1. *Flow is seeded.*
2. *The flow region of interest is illuminated.*
3. *Scattering light from the particles forming the speckle images is recorded by cameras.*
4. *Recordings are analyzed by means of correlation software.*

The scattered light from seeding particles are recorded by a camera (in the case of 3D PIV, two different cameras do the simultaneous recording). The initial position of a particle is recorded on the first frame of the camera right after first laser pulse fires. In general, a typical duration of a laser pulse is about 30 nano seconds in a flow field similar to the current study. Its final position is recorded in the same way on the second frame of the same camera when the second laser pulse fires. The time interval between the two frames is usually determined by the mean flow speed in the area of investigation. The order of magnitude of this time separation between the two frames is "microseconds". Since the displacement of the particle and the time interval between the two subsequent laser pulses are known, the velocity of the particle can be calculated by the simple equation: speed=distance/time. A comprehensive explanation of this technique is given in [12] by R.J. Adrian.

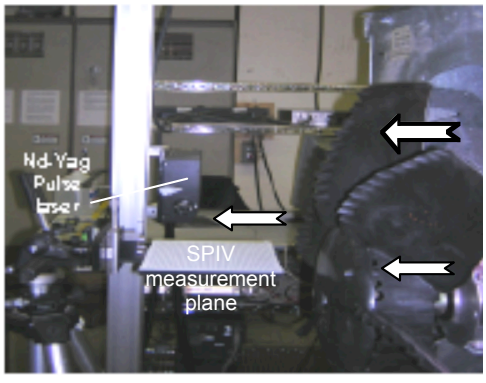

Figure 4: *Calibration plate and fan rotor blades*

In 3D PIV, there is an additional camera viewing the field from a different angle. The two-dimensional image obtained by each camera is slightly different than that of the other, and they are afterwards combined to give three-dimensional velocity information. Stereoscopic vision principles are instrumental in this process of combining the two planar images obtained from the two cameras viewing the same flow-field simultaneously. The data reduction in a stereoscopic PIV system requires the processing of four independent images from the two cameras.

For 3D analysis, the 2D calibration images need additionally to be converted into 3D data by a Direct Linear Transform (DLT) model, in order to calculate the third component of the velocity. Correlation techniques are used to obtain raw vector maps out of image pairs taken during experiments, and a number of calculation methods are used to evaluate these vector maps afterwards. In summary, the three dimensional space defined by the planar measurement area and the finite thickness of the laser sheet is analytically described in relation to the highly distorted images captured by the two CCD chips in each of the two cameras. The distortions observed on the planar CCD images are generated by the angled position of the two cameras. For example, a perfect cube in the measurement space is seen as a distorted cube in each one of the two images generated by the two cameras.

The current study uses high sensitivity cameras that are essential in high speed flow measurements. Two of the 80C60 HiSense PIV/PLIF cameras with 1024 x 1280 pixels are used with 80N57 personality module fitted to processor, and a Nikon Micro-Nikkor 60/2.8 objective, for each camera. The calibration plate and axial fan rotor blades are shown in Figure 4. Initial calibration procedure requires that the laser light sheet generated by the Nd-Yag laser is aligned with the calibration plate carrying a high precision square grid.

EXPERIMENTAL RESULTS AND DISCUSSION

Measurement Domain

In this study, exit flow performance of the axial flow fan was quantified by using Stereoscopic PIV technique. Axial, radial and tangential components of velocity profiles were simultaneously measured near the tip region of the fan under the influence of a few novel tip platform extensions designed throughout this investigation. Most of the SPIV distributions covered a spanwise region from r/R_{tip}=0.6 to r/R_{tip}=1.3. This measurement area corresponds to a region covering the last three quarters of blade height including the tip region flow. The spanwise velocity distributions shown in Figures 8, 9 and 10 are obtained at axial position about 5 cm away from the rotor exit plane. Figure 5 shows the horizontal measurement plane located just downstream of the rotor exit plane. x, y and z directions correspond to radial, axial and tangential (out of plane direction in SPIV laser sheet) directions.

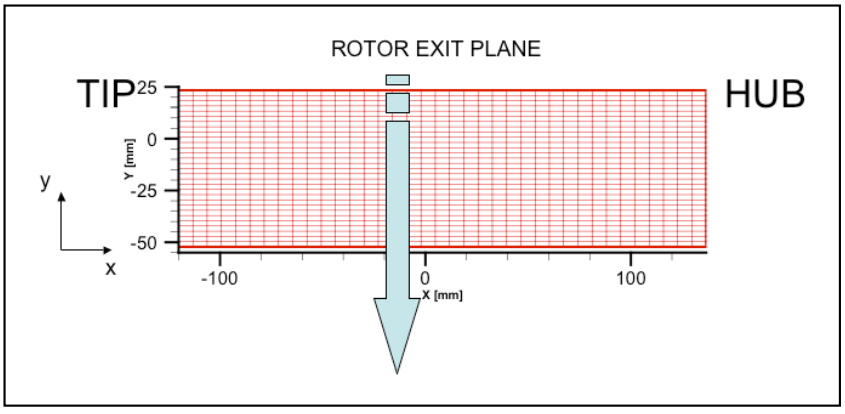

Figure 5: *SPIV measurement plane (horizontal) downstream of the rotor exit*

The radial direction is also marked with r/R_{tip} in order to mark the exact position of the blade root and tip in spanwise distributions of velocity.

Specific Rotor Positions for Phase-locked Measurements

The results from the proposed tip platform extensions are compared to the results obtained from a baseline tip at two different tip clearance levels. All three components of the velocity vector were measured for 7

circumferential locations of the rotor (with respect to the SPIV measurement plane). These locations were chosen by dividing the rotor blade pitch into 7 equiangle regions. These locations can be viewed in Fig.6 . Although the measurements were performed at seven positions, data only from three selected positions are presented. The selected positions include blade tip leading edge, mid-chord and trailing edge (locations 3,4,5).

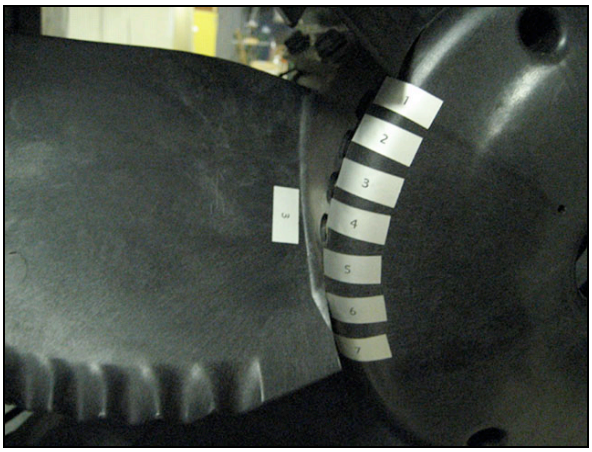

Figure 6: *Rotor positions for phase locking.*

Statistical Stability of the Measurements

Since the mean velocity components in axial, radial and tangential directions are obtained from an ensemble averaging process, the ensemble size is of critical importance in achieving statistically stable mean velocity distributions in SPIV data reduction process. Figure 7 presents the influence of ensemble averaging sample size on the spanwise distribution of the most significant velocity component. The baseline blade tip is used in this experiment with a nominal tip clearance of %1 (of the blade height).

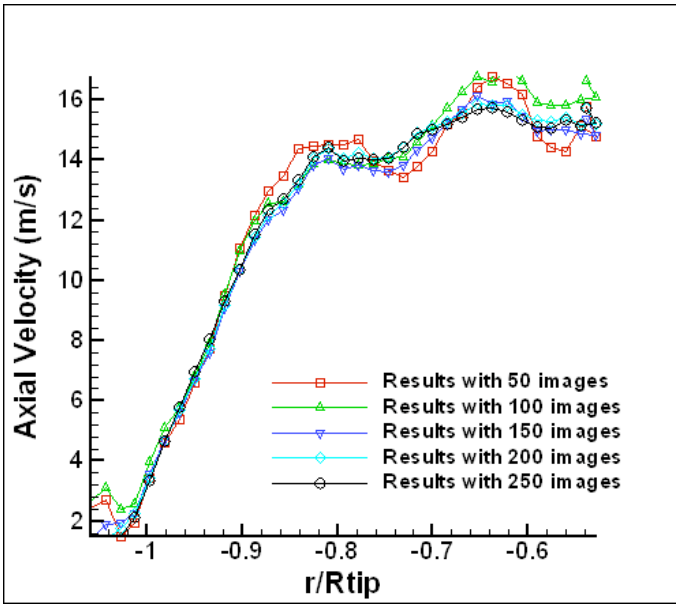

Figure 7: *Influence of sample size in SPIV ensemble averaging*

Figure 7 indicates that an ensemble size of 200 is optimal in achieving a statistically stable average in the current set of experiments. The spanwise region $r/R_{tip}>0.9$ is not significantly influenced from the choice of the ensemble averaging sample size. The sample sizes of 150, 200 and 250 produce very similar spanwise distributions in this region near the tip. A typical experimental uncertainty in the current SPIV based velocity

measurements is estimated to be less than 0.6 % of the mean value (±0.1 m/s). All SPIV experiments are conducted using an ensemble averaging sample size of 170.

Tip Platform Extension Design

An effective control of tip leakage flow was achieved using different tip platform extensions. The term "*control of tip leakage flow*" could be defined as the "*minimization of tip leakage flow mass flow rate*". All of the tip platform extensions used in this study were evaluated at two different tip clearance values of 0.1 inch and 0.135 inch corresponding to %1 and %1.35 of the blade height.

The main main goal of this study is to minimize the tip leakage mass flow rate by interfering with the flow on the pressure side corner of the blade tip region. It is likely that a new static pressure distribution near the blade tip section is defined by the novel tip platform extension designs shown in Fig. 8 . The impact of the suggested tip platform extensions are visible in the velocity magnitude animations obtained from the tip region. The animated near-tip flow velocities obtained from the phase-locked SPIV measurements clearly show the "*velocity magnitude calming*" effect of tip platform extensions. It is also highly visible that the tangential velocity components induced by the baseline tip are almost eliminated by effective tip platform design. This observation is very clear especially near the tip diameter of the rotor exit flow

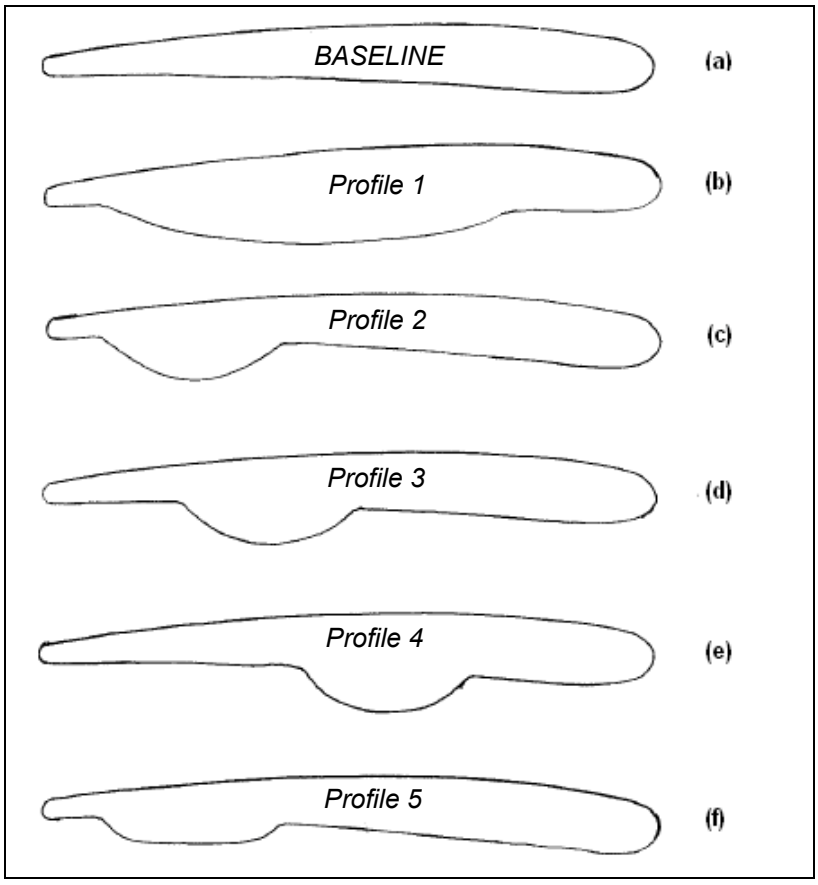

Figure 8: *Novel tip platform extensions for tip leakage control*

The tip platform extensions were designed by adding different "*pressure side bumps*" to the base profile as shown in Fig.8. Initially, a wide bump between trailing edge and leading edge was suggested as Profile 1. The maximum width of the bump was chosen as the same as the thickness of the airfoil at the bump centerline location. Three more tip platform extensions were derived from Profile 1 by dividing the wide bump of Profile 1 into three almost equal chordwise sections. The three new tip platform extensions are termed Profile 2 (near the trailing edge), Profile 3 (middle of the wide bump) and Profile 4 (almost mid-chord). The bump maximum widths were kept the same. Profile 5 is a derivative of the trailing edge bump named as Profile 2. This specific tip platform extension uses a relatively small platform following the profile of the baseline design. The external contour of Profile 5 is almost parallel to the baseline profile except the areas where blending is suggested. The thickness of the platform extended on the pressure side of the blade is

about 0.030 inch (0.762 mm) for all designs used in this investigation. Only one rotor blade at a time out of seven blades was retrofitted with a suggested design. Each experiment had six baseline blades and a suggested tip platform extension as the seventh blade. The effective clearance was kept the same for all seven blades.

Figures 9,10,11 show results of the exit flow measurements of the axial flow fan at the highest volumetric flow rate condition defined as (340m^3/min, 32 Pa) . Fig. 12 complements these results from a data set obtained at the minimum mass flow rate condition where the pressure loading is maximum (80m3/min, 140 Pa). All the velocity profiles are plotted at 1.811 inch (46 mm) downstream of the fan.

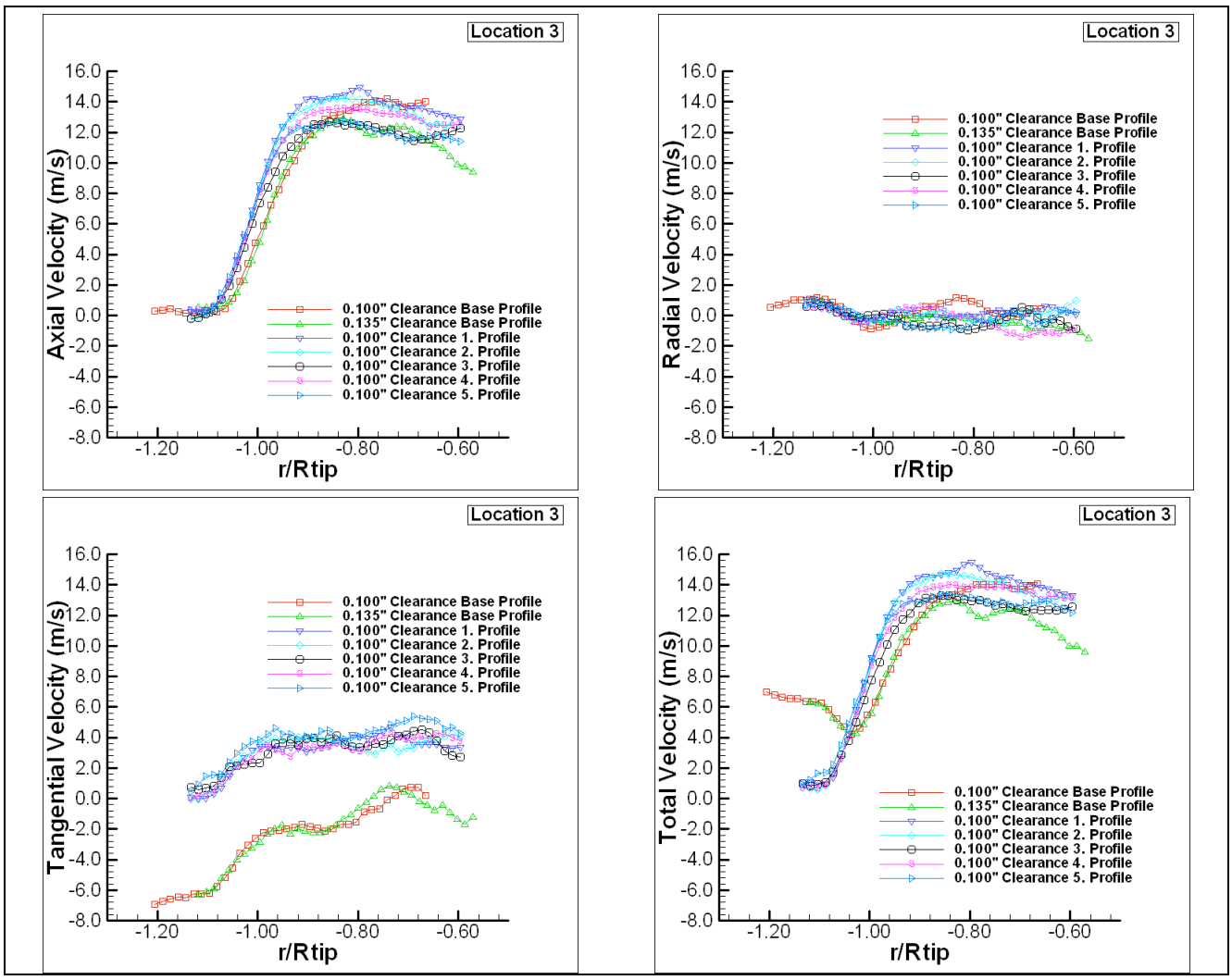

Figure 9: *Velocity Profiles measured at location 3*

Total Velocity and all Three Components at Rotor Exit

In addition to the magnitude of the velocity vector (total velocity); the radial, tangential and axial components of the velocity vector at the exit of the rotor is provided in Fig. 9 in function of the spanwise distance. It should be noted that the radial component is positive in radially inward direction. The absolute magnitude of r/R_{tip} is used for convenience throughout this manuscript. In the region where $r/R_{tip}>0.9$, the two base profiles show very similar trends. 0.100" Clearance Base Profile and 0.135 " Clearance Base Profile generates two different tip vortices. The total velocity is significantly reduced in the core of the passage where r/Rtip<0.9 when tip clerance is high at 0.135 " level. The significant momentum deficit occuring in the core of the two tip vortices from the two baseline tips greatly influence the core flow and reduce the mean kinetic energy even after they are mixed with the wake fluid that is also modified by the serrated trailing edge geometry as shown in Figures 2 and 6. This observation indicates that a significant momentum deficit in the

core of the passage vortex exists because of the tip vortex and this deficit becomes worse when the clearance increases. Even under strong mixing conditions induced by the wake fluid of originating from the serrated trailing edges the direct impact of the baseline tip vortex is visible in the measured total velocity. The radial component for all cases as shown in Fig. 9 are all very small magnitudes around ± 1 m/s. There is no significant influence of the level of baseline clearance or the type of the tip treatment on the magnitude of the radial component.

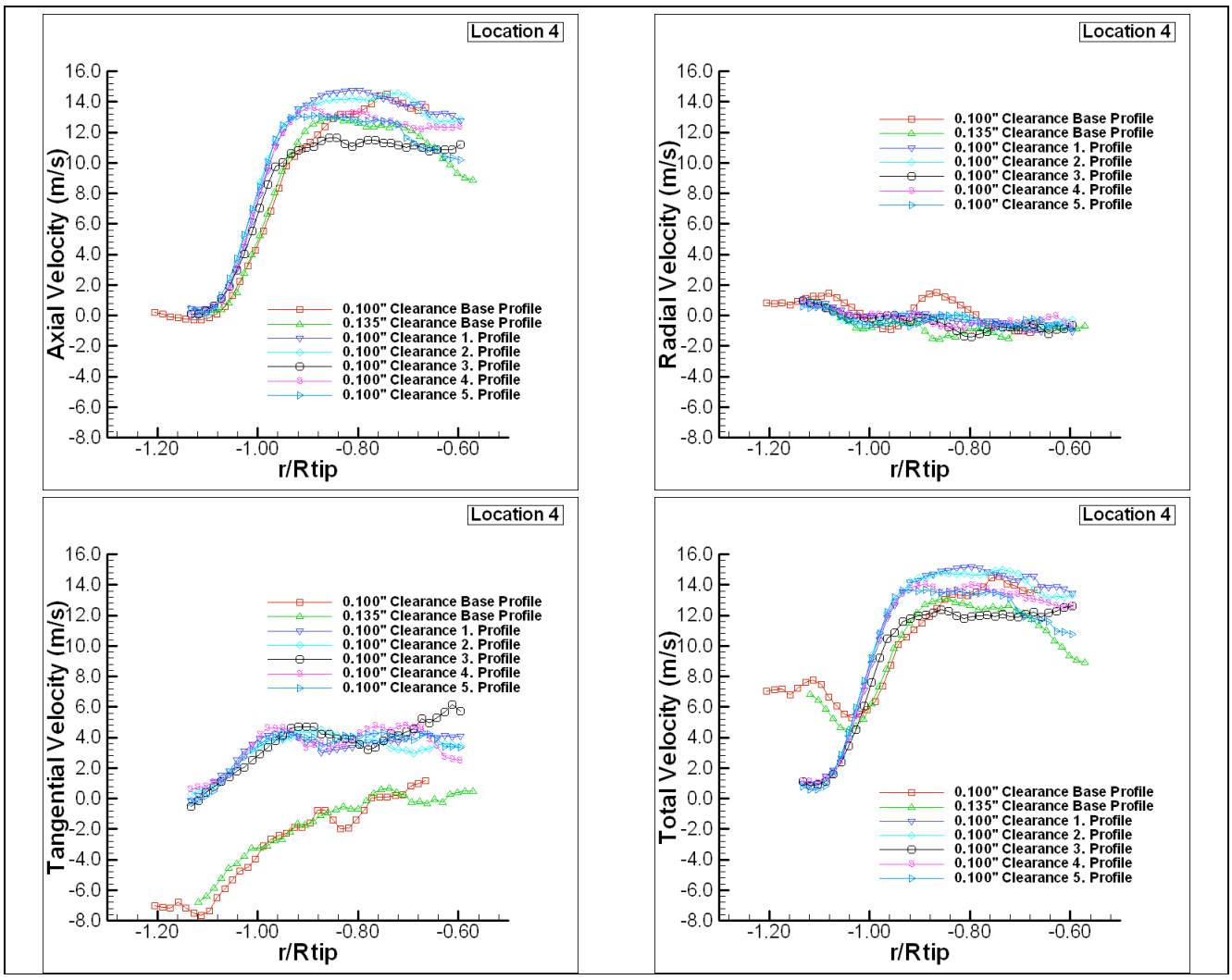

Figure 10: *Velocity Profiles measured at location 4*

When the axial velocity component is compared to the total velocity, a striking observation in the tip region is apparent. The total velocity for the baseline tips is much higher than the axial component where $r/R_{tip}>1.05$. Since the radial components are extremely small for all tip shapes, one can infer that the significant difference between the baseline tips and the treated tips is due to a strong change in the tangential component of the velocity vector. The distribution of the tangential component clearly shows that difference in the region where $r/R_{tip}>0.6$. The five tip platform extensions shown in Figure 6 clearly participate in the reduction of the tangential component in the last three quarters of the blade height. The elimination of the tangential component is the most effective near the tip. This influence is slightly reduced when one moves away from the tip in radially inward direction. The reduction in the amount of swirl or tangential component near the tip region is about 4-5 m/s on the average. The magnitude of the swirl component that is inherent to baseline tips is about one third of the total velocity existing in the core of passage.

It is clear that the new tip platform extension devices can be highly instrumental in reducing the amount swirl coming out of the rotor in the rotor exit area. This feature is certainly a benefit in terms of the energy efficiency of the axial flow fan when the fan is operated on its high volumetric flow rate (low pressure rise) point. Another significant benefit is the improvement of the aeroacoustic field through reductions in the amount of swirl contined in rotor exit flow. The tip platform extensions help to reduce the tip leakage mass flow rate and its momentum deficit via local static pressure modifications near the tip region.

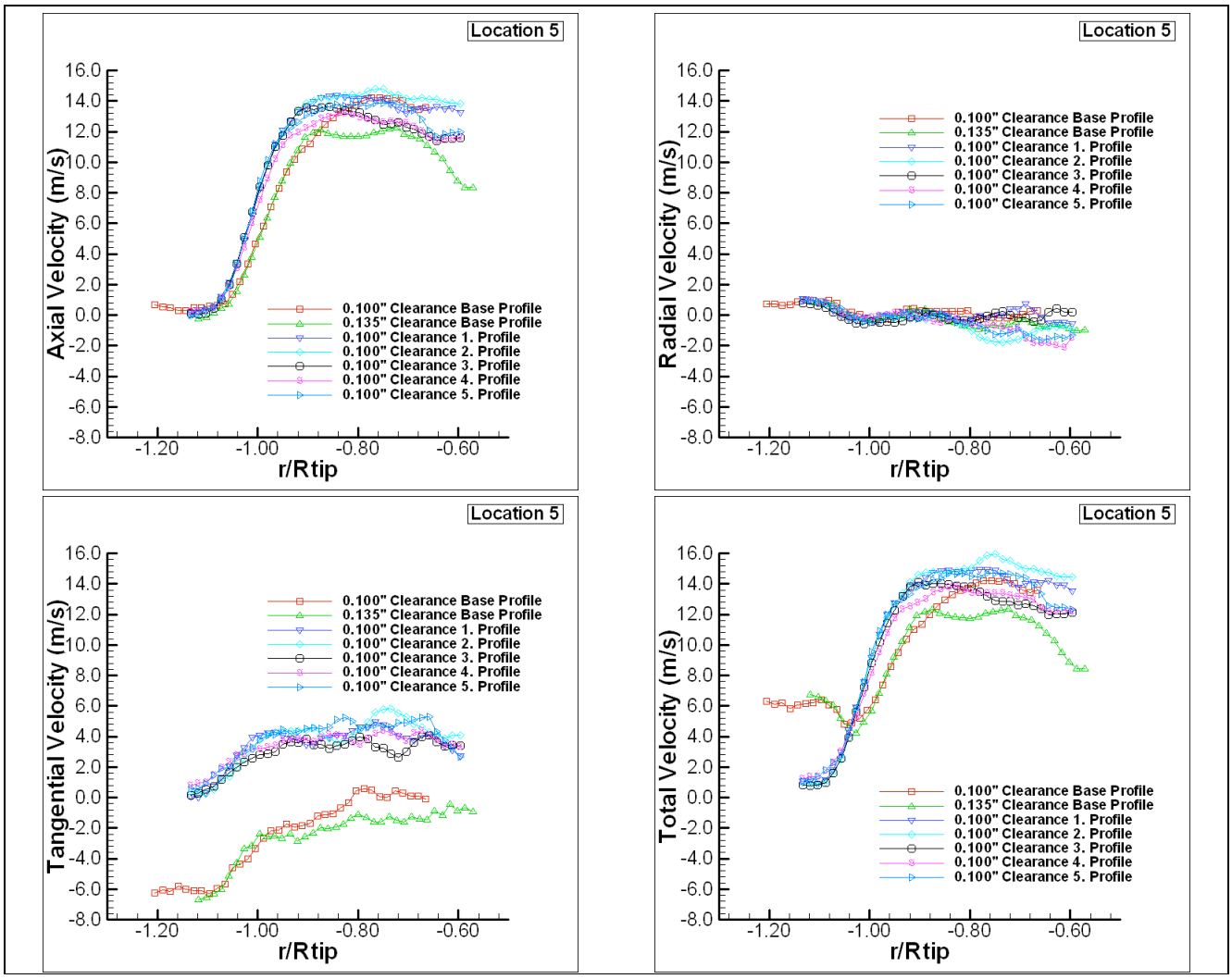

Figure 11: *Velocity Profiles measured at location 5*

The Profile 1 and Profile 2 are the two profiles with the highest total velocity in the core of the passage exit flow. It seems that the maximum width of the bump is an important parameter in designing the tip de-sensitization geometry. The Profile 2 and 5 cover almost the same chordwise locations. The only difference between the two is the maximum width of the bump. Figures 9, 10 and 11 clearly shows that the recovery of the axial velocity component and elimination of the tangential component is much effective with Profile 2 than with Profile 5. Figures 9, 10 and 11 show that the features observed in Fig.9 for location 3 repeat for other positions of the rotor (location 4, 5, and 6). Although there are slight differences at different rotor positions, the general nature of this dicussiion does not change.

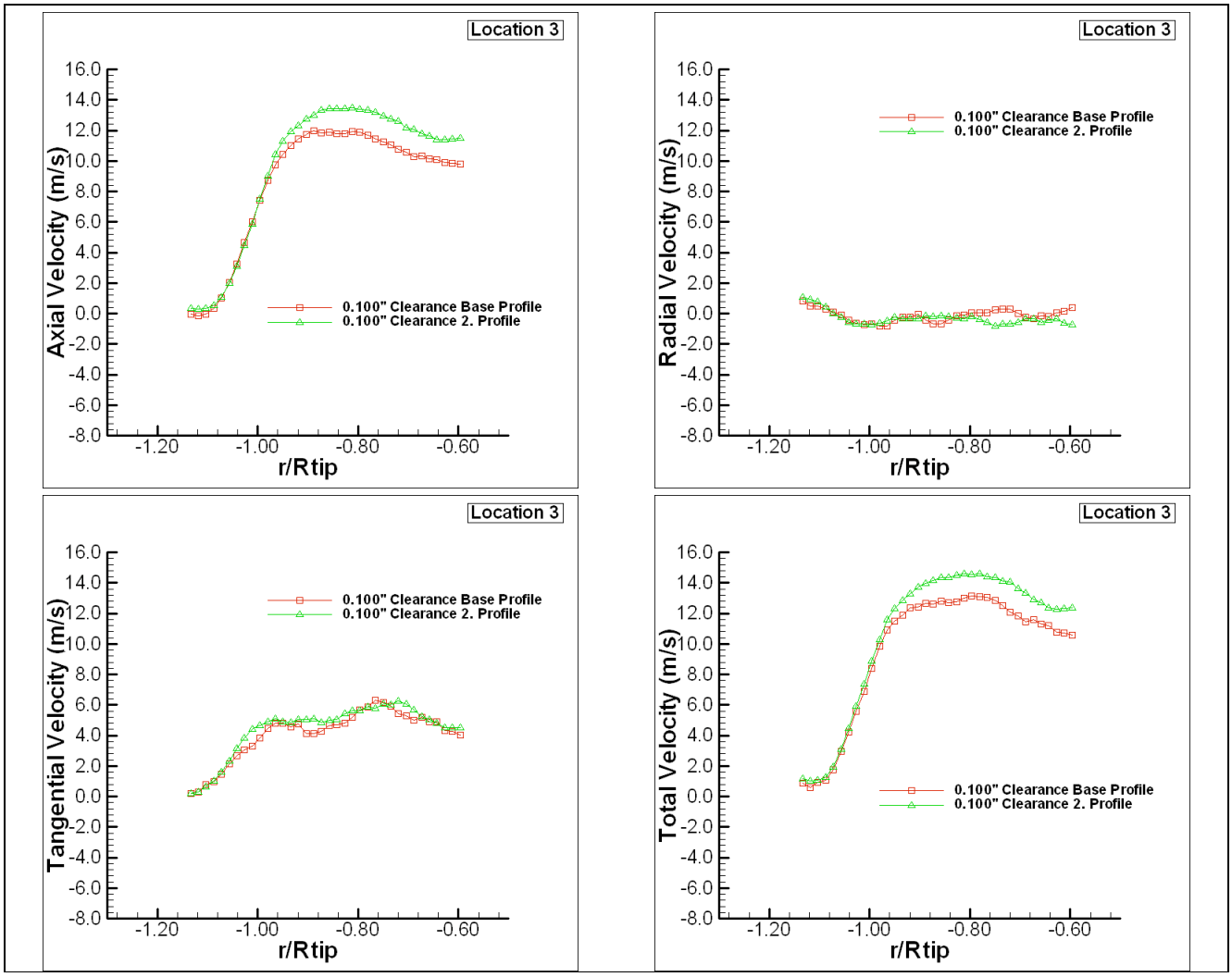

Figure 12: *Velocity Profiles measured at location 3 with pressure load*

An interesting tip treatment experiment could be performed by operating the fan at its highest presure point by reducing the volumetric flow rate using a perforated steel plate at the mock-up inlet section. The specific perforated plate with an open area ratio of % 19 indicated that the gains in axial velocity component at the core of the exit flow still exists with Profile 2. Figure 12 shows that tangential and radial velocity components from Profile 2 are very similar to the baseline profile at the same effective clearance value of 0.100" (%1). However the elimination of the tangential component observed in high volumetric flow rate experiments does not occur under high pressure rise conditions. There is a consistent 2 m/s increase in axial (or total) velocity throughout the blade span when r/R_{tip}>06. Under high loading conditions the swirl component is minimal even with a baseline tip. Therefore the tip platform extensions perform their function by minimizing the tip leakage flow mass flow rate near the blade tip. This effect eventualy provides the gain in axial component. On the average the gain in total velocity magnitude at the rotor exit is about %17 through out the balde span. This type of gain in mean kinetic energy of fan exit flow is expected to contribute to the energy efficiency of the fan.

CONCLUSIONS

Novel tip platform extensions for energy efficiency gains and aeroacoustic improvements were designed for an axial flow fan where wake mixing is already enhanced with a serrated trailing edge design.

Five different tip platform extensions were introduced especially on the pressure side of the fan blades.

It is possible to reduce tip leakage mass flow rate using the novel tip platform extensions. Profile 2 showed the best tip treatment character out of the five new tip platform extensions designed in this investigation.

Tip treatment experiments performed at high volumetric flow rate/low pressure rise clearly showed the minimization of tip vortex mass flow rate by reducing the tip region tangential components significantly.

The tip platform extensions on the pressure side have proven to be effective swirl reducing devices at the exit of the fan. The magnitude of this reduction is about one third of the rotor exit total velocity in the core of the passage exit.

The reduction in tangential component near the tip is expected to reduce the aeroacoustic signature of the fan unit when it is operated under high mass flow rate/low pressure conditions.

The reduction of tip leakage mass flow rate produced enhanced total velocity values between the mid-span and the tip at the passage exit.

Experiments performed at the highest presure point by reducing the volumetric flow rate using a perforated steel plate at the mock-up inlet section also showed significant tip leakage control for the fan. However the elimination of the tangential component observed in high volumetric flow rate experiments does not occur under high pressure rise conditions.

Under high loading conditions the swirl component is minimal even with a baseline tip. There is a consistent 2 m/s increase in axial (or total) velocity throughout the blade span when $r/R_{tip}>06$.

Tip platform extensions perform their function by minimizing the tip leakage flow mass flow rate near the blade tip even under the high loading conditions. This effect eventualy provides the gain in axial component.

On the average the gain in total velocity magnitude at the rotor exit is about %17 through out the blade span. This type of gain in mean kinetic energy of fan exit flow is expected to contribute to the energy efficiency of the fan.

References

[1] Lee,G.H., Baek, J.H. and Myung, H.J. , "*Structure of Tip Leakage in a Forward-Swept Axial-Flow Fan*," Flow,Turbulence and Combustion, Vol. 70, pp:241-265, Jan 2003.

[2] Jang, C.M., Frukawa, M. and Inonue, M., "*Analysis of Vertical Flow Field in a Propeller Fan by LDV Measurements and LES- Parts I,II* , ASME J. Fluids Eng., Vol. 123, pp:748-761, 2001.

[3] Storer, J. A., Cumpsty, N. A., *Tip Leakage Flow in Axial Compressors*, Journal of Turbomachinery, Vol. 113, April 1991.

[4] Lakshminaraya, B., Zaccaria, M. and Marathe, B., *The structure of Tip Clearance Flow in Axal Flow Compressors*, ASME Journal of Turbomachinery, Vol 117, pp:336-347, 1995.

[5] Reynolds, B., Lakshminaraya, B., and Ravindranath, A., "*Characteristics of Near Wake of a Fan Rotor Blade*," AIAA Journal, Vol 17, pp:959-967, Sept. 1979.

[6] Ravindranath, A., and Lakshminaraya, B., "*Mean Velocity and Decay Characteristics of Near and Far-Wake of a Compressor Rotor Blade of Moderate Loading,"* Journal of Engineering for Power, Vol. 102, pp:535-547, July 1980.

[7] Myung, H. J. and Baek, J. H. , "*Mean Velocity Characteristics Behind a Forward- Swept Axial-Flow Fan* , JSME Int. J., Ser. B, Vol. 42, pp:476-488.

[8] DANTEC, "*Particle Image Velocimetry: An Informative Seminar on PIV Techniques for Whole Field Flow Measurements*,".

[9] DANTEC, "*FlowMap 3D-PIV System-Installation & User's Guide*,".

[10] DANTEC, "*FlowMap Particle Image Velocimetry Systems - Integrated Real-time PIV Instrumentation*," ,1998.

[11] DANTEC, "*FlowMap Particle Image Velocimetry Instrumentation-Installation & User's Guide*", 2000.

[12] Adrian, R.J., *,"Particle Imaging Techniques for Experimental Fluid Mechanics*," Ann. Rev. Fluid Mech.*,* Vol. 23, pp. 261-304, 1991.

[13] Kahveci, H.S., "*Implementation of a Stereoscopic PIV In Rotating Machinery Including Helicopter Rotor Flows",* M.Sc.thesis, The Pennsylvania State University, July 2004.

[14] Yoon, J.H. and Lee, S.J., *"Stereoscopic PIV Measurements of Flow Behind an Isolated Low-speed Axial Fan,"* Experimental Thermal and Fluid Science, Vol. 28, pp:791-802, 2004.

[15] Yen, S.C. and Yen, F.K.T., "*Exit Flow Field and Performance of Axial Flow Fans*," Journal of Fluids Engineering, Vol. 128, pp:332-340, March 2006.